water

MDPI

Article

Biosorption of Iron-Contaminated Surface Waters Using *Tinospora cordifolia* Biomass: Insights from the Gostani Velpuru Canal, India

Penupothula Raju [1,2,3,*], Fasil Ejigu Eregno [1], Rajnish Kaur Calay [1], P. Ramakrishnam Raju [2] and Thokhir Basha Shaik [2]

[1] Department of Building Energy and Material Technology, Faculty of Engineering Science and Technology, UIT The Arctic University of Norway, 8514 Narvik, Norway
[2] WET Research Center, SRKR Engineering College (A), Bhimavaram 534204, India
[3] Department of Civil Engineering, SRKR Engineering College (A), Bhimavaram 534204, India
* Correspondence: penupothularaju6993@gmail.com or penupothula.raju@uit.no

Abstract

The contamination of water bodies with heavy metals from various anthropogenic sources has become a prominent global issue. New industrial establishments and rapid urbanization have led to heavy metal intrusion into various surface water bodies, deteriorating water quality and causing numerous health issues for people consuming it. Removal of heavy metals from water is a complicated and costly process; hence, researchers are adopting various techniques to remove them naturally. This paper assesses the performance of a biosorption technique to remove heavy metal iron from Gostani Velpuru Canal, India. The techniques involved using biomass of *Tinospora cordifolia* in the form of green stem (GSB), dry stem (DSB), and extracted powder (PB). The efficiency of iron removal was measured from water samples collected diurnally from the canal. The study focused on the variations of *T. cordifolia* biomass combinations in iron absorption using static and agitated methods. The results indicated that PB with agitation had the highest mean iron removal efficiency of 72.43%, followed by DSB (41.77%) and GSB (35.32%) in the collected GVC samples. These findings suggest that *T. cordifolia*, regardless of its form, can be used for diverse water resource applications.

Keywords: heavy metal; *Tinospora cordifolia*; biomass; biosorption; iron; water; pollution

check for updates

Academic Editor: Yanshan Cui

Received: 10 September 2025
Revised: 13 October 2025
Accepted: 17 October 2025
Published: 21 October 2025

Citation: Raju, P.; Eregno, F.E.; Calay, R.K.; Raju, P.R.; Shaik, T.B. Biosorption of Iron-Contaminated Surface Waters Using *Tinospora cordifolia* Biomass: Insights from the Gostani Velpuru Canal, India. *Water* **2025**, *17*, 3020. https://doi.org/10.3390/w17203020

Copyright: © 2025 by the authors. Licensee MDPI, Basel, Switzerland. This article is an open access article distributed under the terms and conditions of the Creative Commons Attribution (CC BY) license (https://creativecommons.org/licenses/by/4.0/).

1. Introduction

Global heavy metals originating from natural and anthropogenic source contamination in aquatic environments are growing problems [1,2]. Mining, municipal waste, industry, agriculture, aquaculture and stormwater runoff contribute to heavy metal accumulation in water bodies [2–4]. The concentration of heavy metals in water bodies depends on the type of rock or soil along the watershed [2]. Heavy-metal-induced water pollution harms aquatic ecosystems posing health risks to animals and humans due to transfer through the food chain [1,5]. Even at low concentrations, heavy metals present in surface water can be toxic to both organisms and humans [4]. In developing countries the heavy metal concentrations were found to be higher than the WHO (World Health Organization) and USEPA (United States Environmental Protection Agency) limits compared to developed countries of Europe and North America [5].

A study on heavy metal toxicity in Indian rivers [6] by FSSAI (Food Safety and Standards Authority of India) and CWC (Central Water Commission) discovered that out of 688 water quality monitoring stations, 240 exceeded the acceptable limit for iron concentration set by BIS (Bureau of Indian Standards): 10500-2012 [7].

Compared to other heavy metals (arsenic, cadmium, chromium, copper, nickel, lead, and zinc), iron concentration was found to be higher [6]. Excessive iron concentration in wastewater is harmful to the environment. Iron contamination in water results from anthropogenic sources such as waste effluents of cast iron and steel industries, iron coagulants, cookware, and the corrosion of old and galvanized iron pipes during water distribution [8–11]. Microorganisms like Schizomycetes and iron-oxidizing bacteria form hydrogen sulphide that corrodes pipes [12].

Whereas iron is essential for the human body in limited concentrations and drinking water is the primary source of iron, its ingestion in large amounts results in hemochromatosis, a condition where normal regulatory mechanisms fail, causing tissue damage. Iron bioaccumulation causes rapid increases in respiration, pulse rate, blood vessel coagulation, hypertension, and drowsiness [2,11]. Excess iron in the human body escalates the risk of various cardiovascular diseases and oxidative stress [13]. Therefore, the USEPA and BIS have approved iron content for drinking water of 0.3 mg/L or ppm [7,8] and imposed a maximum permissible limit in wastewater of 3.0 mg/L [14].

In this study, we studied the Godavari region and observed that the overuse of chemical fertilizers has contaminated the agricultural soil with heavy metals like iron, cadmium, and zinc [15]. These metals easily enter water bodies as agricultural discharge. It is known that heavy metals do not naturally degrade in the aquatic environment through natural processes [3]. Therefore, techniques like reverse osmosis, catalytic oxidation, ion exchange, solvent extraction and electrochemical treatment methods are necessary for their removal [16,17]. These techniques are often expensive and generate significant amounts of liquid waste and sludge; thus, they are not feasible solutions for industries and water treatment plants.

Several biomasses such as living or non-living aquatic plants have the capability to absorb heavy metals [18]. These aquatic plants play a crucial role in accumulating metals by reducing stream water velocity and promoting precipitation [15,19]. Researchers have studied the biosorption of heavy metals and the removal of pollutants using a wide variety of plant species [18–24]. Biosorption involves the binding of metal ions to the surface of a biosorbent [25,26] (like a plant); the ability to accumulate metals varies between plant species and is associated with their morphology and growth [19].

Tinospora cordifolia is a climbing or twining plant which belongs to the menispermaceae family [27], and is found in tropical regions of India, China, Sri Lanka, and Bangladesh. This plant is rich in alkaloids, terpenes, and phenolic compounds, with functional groups such as hydroxyl (–OH), carbonyl (–C=O), etc., making it capable of hyperaccumulating metals [28]. Traditional claims of *T. cordifolia*'s potential to treat various ailments such as fever, asthma, diabetes, blood pressure issues, malaria, and dengue have been scientifically validated. *T. cordifolia*'s antibacterial, antimicrobial, antioxidant, antitoxic, antifungal, anti-diabetic, anti-stress, and anticancer resistance makes it a desirable plant for various pharmacological applications [27–33]. It is quoted as 'medhya rasayana' in Ayurveda, known for its learning and memory enhancement properties and its potential for treating vertigo [30], and hence, it is also termed as amruthavalli, recommended for enhancing body resistance, promoting longevity, and acting as an anti-stress and adaptogen [32]. Clinical tests have shown that the plant's anti-stress and tonic properties have shown significant responses in children with moderate behaviour disorders and mental deficits, resulting in improved IQ levels [30,34]. The morphology of *T. cordifolia*, including its

leaves, roots and stem, is documented to be useful in ethnobotanical surveys conducted by ethnobotanists [31]. The stem is widely recognized as the most effective and beneficial part of the plant in Ayurvedic medicine [27]. The aqueous extract of *T. cordifolia* stem has antioxidant properties; it showed no harmful effects or deaths in acute poisoning tests, even at a high dose of 9 g/kg body weight [28,29,33]. *T. cordifolia* biomass was found to be effective in reducing fluoride levels in drinking water at neutral pH [35].

The derived biomass of *T. cordifolia* exhibited excellent characteristics of adsorption of iron (III) using SEM-EDS, EDX, and powder XRD analysis [16]. Despite having a wide range of applications, limited research has been carried out on the impact of *T. cordifolia* in removing heavy metal contamination [21] in flowing water bodies. And to our knowledge, there are no investigations on the efficiency of iron removal by *T. cordifolia* biomass along with its life cycle assessment in the literature. This study focuses on the biosorption efficiency of *T. cordifolia* biomass in reducing iron concentration in three stages (green, dry and powder form) and their significant sustainable impact on surface water bodies on a macroscopic scale.

2. Materials and Methods

2.1. Study Area and Location

Gosthani Velpuru Canal (GVC) is one of the major canal systems in the western Godavari delta in southern India. This canal has various point and non-point sources of pollution due to various anthropogenic activities like domestic sewage, industrial, poultry, and agricultural and aquacultural discharges along its stretch [12]. Ten such locations on this canal were identified as hotspots, marked as A, B, C, D, E, F, G, H, I and J in Figure 1, and samples were drawn from these hotspots simultaneously at regular intervals during the diurnal times of a day. Laboratory-scale experiments were conducted using a UV–visible spectrophotometer to assess the iron removal efficiency of three different biomass forms of the *T. cordifolia* plant from all the diurnal samples. These experiments involved comparison of iron removal efficiency of the plant biomass with the standard, and blank samples and were tested under both agitated and static (non-agitated) conditions for all samples, with the biomass with agitation representing the efficiency of *T. cordifolia* plant in turbulent flow conditions that occur in streams and rivers, and biomass without agitation representing steady flow conditions that occur in ponds and water pools.

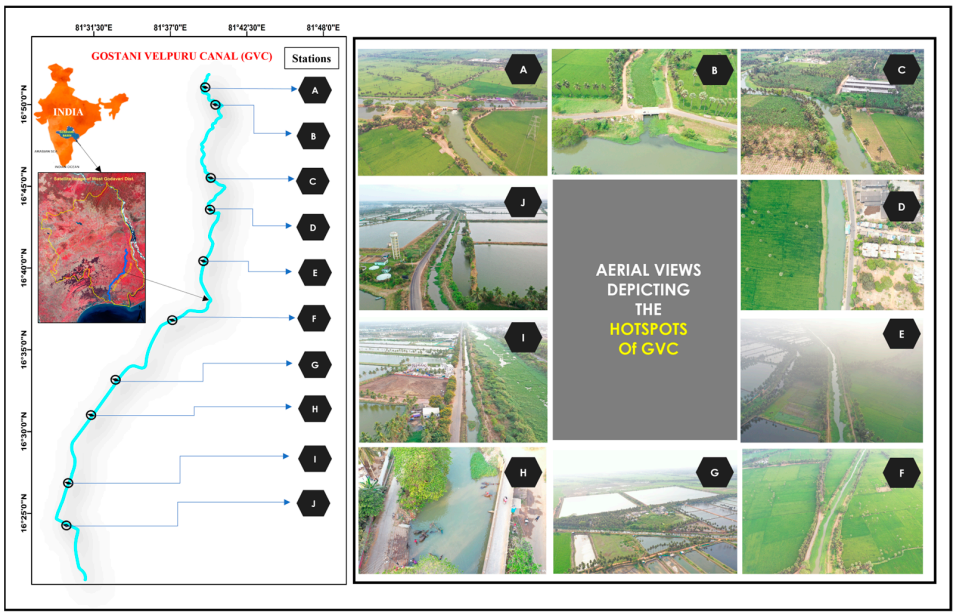


Figure 1. GVC hotspots and aerial view of each hotspot.

2.2. Water Sampling and Analysis

A preliminary study taking water samples across the GVC stream was conducted to find heavy metal contamination. Laboratory analysis confirmed the concentration of heavy metals such as iron (Fe), copper (Cu), cadmium (Cd), zinc (Zn), and manganese (Mn) found in previous studies of the Godavari river [6]. However, iron (Fe) contamination was found to be predominant amongst other metals. Therefore, iron was chosen for the process of biosorption through *T. cordifolia* biomass. Six water samples at each station were collected at diurnal times, starting from 8:00 AM to 6:00 PM at an interval of 2 h between each sample, marked as T1, T2, T3, T4, T5 and T6. All the samples were collected in the pre-monsoon season to avoid turbid waters during monsoon and post-monsoon seasons. Samples collected for the analysis were tested in the laboratory for parameters like pH, TDS, alkalinity, TH (total hardness), chlorides, sodium, COD, DO, and iron according to the standard methods established by the American Public Health Association (APHA) [36]. Table 1 shows the locations of the 10 hotspots and the diverse identified sources of pollution at each hotspot.

Table 1. Sampling locations and potential sources of pollution on the GVC.

Station Code	Latitude	Longitude	Identified Potential Sources of Pollution (%)				
			Agriculture	Aquaculture	Industries	Domestic Sewage	Poultry
A	16.8531472° N	81.6795417° E	100	-	-	-	-
B	16.8348222° N	81.6930083° E	20	20	20	20	20
C	16.7632139° N	81.6760444° E	33.33	-	33.33	33.33	-
D	16.7313222° N	81.6757361° E	33.33	-	33.33	33.33	-
E	16.6853500° N	81.6656528° E	25	25	-	25	25
F	16.6287917° N	81.6306889° E	50	50	-	-	-
G	16.5651222° N	81.5649194° E	33.33	33.33	33.33	-	-
H	16.5370778° N	81.5409972° E	33.33	33.33	-	33.33	-
I	16.4750806° N	81.5152972° E	25	25	25	25	-
J	16.4360111° N	81.5157583° E	20	20	20	20	20

2.3. Collection and Preparation of T. cordifolia Biomass

To validate the biosorption efficiency of *T. cordifolia* biomass in removing iron, *T. cordifolia* plant creepers were collected from the banks of the GVC.

- Green Stem Biomass (GSB): Fresh *T. cordifolia* creepers were collected and washed with distilled water to ensure they were free from dust and impurities. The stems were then chopped to specific dimensions for the intended use [21,31,32].
- Dry Stem Biomass (DSB): The *T. cordifolia* creeper stems were cut, and leaves and skin were removed and then dried in an oven at 100 °C until moisture-free. The dried stems were then cut into desired lengths [16,31].
- Powdered Biomass (PB): Fresh *T. cordifolia* stems were cut into small pieces and dried at 65 °C for 6 h [16,21], with a total weight of 600 g. They were combined with 2400 mL of water (four times the weight of the stems) in a beaker, filtered, and allowed to settle [37,38]. The residual component after desiccation, which was creamish brown in colour with a characteristic odour, was collected [31].

The life cycle assessment of *T. cordifolia* encompasses these three biomass types, as shown in Figure 2. The three biomass combinations were categorized into biomass with

agitation and biomass without agitation. The plant biomass was subjected to optimization of various parameters such as equilibrium time, dosage, concentration and the applicable biosorption models.

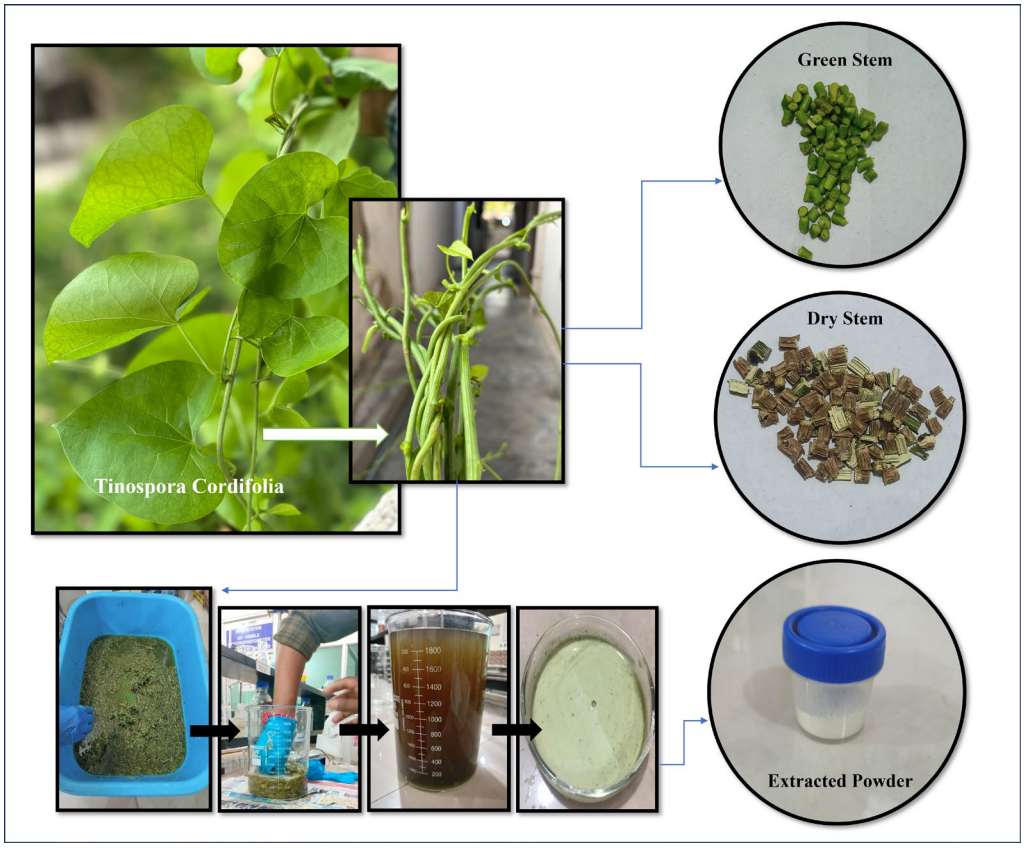


Figure 2. *Tinospora Cordifolia* biomass preparation.

2.4. Detection Method of Iron

Iron present in surface waters can be detected in ferrous form (Fe^{2+}) or ferric form (Fe^{3+}) [39]. (Fe^{2+})/iron (II) ions combine with 1,10-phenanthroline to produce an orange-red complex, ferrous ortho-phenanthroline $[(C_{12}H_8N_2)_3Fe]^{2+}$, as shown in Figure 3. Maximum absorbance is exhibited at a wavelength (λmax) of 510 nm, which can also be detected using a UV–visible spectrophotometer. The colour intensity is unaffected by acidity throughout the pH range of 2 to 9 and remains stable over longer periods. Initially, all (Fe^{3+})/iron (III) ion concentrations may be reduced to iron (II) using a hydroxylamine solution [40,41]. So, all forms of iron can be converted and detected using this method.

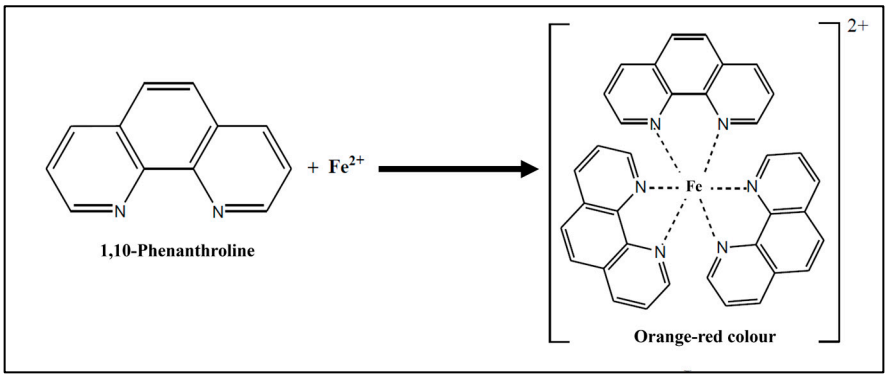


Figure 3. Reaction of 1,10 phenanthroline and iron (II) [41].

The calibration curve for iron concentration vs. absorbance was plotted. The plot and linear equation (y = mx + c) were used to convert absorbance to concentration. The calibration graph can be used to calculate iron concentration in water samples.

2.5. Control Conditions and Reagent Requirements for Iron Detection

The reagents used in iron detection were concentrated HCl, hydroxylamine solution, ammonium acetate buffer solution, phenanthroline solution, and stock iron solution [41]. Control conditions were set for all *T. cordifolia* biomass combinations with 10 mL of Millipore water to check if the plant biomass released iron content into the water [22]. Test tubes were filled with an iron standard and 100, 200 and 300 mg of *T. cordifolia* biomass in control and without control conditions. Initial readings were taken, and the samples were diluted in Eppendorf tubes and agitated (for agitated samples only) at 152 RPM and 37 °C, after which the absorbances of all samples were recorded. As shown in Table 2, 4ppm was used as the standard concentration of iron across all biomass combinations, because most samples of GVC fell just below the 4 ppm range, and the 3 ppm permissible limit for iron in wastewater [14] falls under this limit.

Table 2. Sample codes, control conditions and iron standards of *T. cordifolia* biomass.

S.no	GSB Sample Codes	DSB Sample Codes	PB Sample Codes	Iron Standard (ppm)	Volume (mL)	TC Biomass
1.	GSB-1	DSB-1	PB-1	4	10	Yes
2.	GSB-2	DSB-2	PB-2	4	10	Yes
3.	GSB-3	DSB-3	PB-3	4	10	Yes
4.	GSB Blank	DSB Blank	PB Blank	4	10	No
5.	GSBC-1	DSBC-1	PBC-1	-	10	Yes
6.	GSBC-2	DSBC-2	PBC-2	-	10	Yes
7.	GSBC-3	DSBC-3	PBC-3	-	10	Yes

GSB/DSB/PB-1/2/3 indicates green stem, dry stem, and powdered *T. cordifolia* biomass of 100/200/300 mg combinations for 10mL samples, and GSBC/DSBC/PBC-1/2/3 indicates the control conditions.

The actual concentration of iron is obtained by deducting the concentration of iron in the sample from the concentration of iron in the control conditions of each biomass form.

2.6. Removal Efficiency Calculation of T. Cordifolia Biomass

The removal efficiencies of iron by *T. cordifolia* were estimated based on the initial concentrations of iron in raw water [17] by using the following formula.

$$(\%)\ \text{Removal efficiency}\ (R_e) = ((C_i - C_f) \times 100)/C_i \quad (1)$$

where C_i and C_f are the concentrations of iron in raw and treated water, respectively.

3. Results and Discussion

The physico-chemical analysis of all the samples was performed in the laboratory as per standard methods [7,36]. The mean concentrations of the parameters are shown in Table 3. The parametric mean concentrations of pH, TDS, ALK, chlorides, TH, COD, and sodium increased from upstream to downstream, indicating the contamination of the canal by anthropogenic activities. Similarly, the decrease in the concentration of DO from upstream to downstream indicates the deterioration of water quality along the canal stretch.

The other parametric distributors, like standard deviation, maximum, and minimum of the samples, can be found in Table S1 of the Supplementary Material.

Table 3. Parametric mean concentrations at each station.

Station Code	Mean Concentration of Various Parameters at Each Station							
	pH	TDS	ALK	Chlorides	TH	COD	Sodium	DO
A	7.74	174.93	64.81	24.99	131.07	54.35	14.45	4.71
B	7.81	186.61	74.83	29.71	129.87	65.27	15.20	4.50
C	7.79	219.92	78.03	44.80	156.04	85.35	23.69	5.31
D	7.77	231.64	72.94	48.00	141.63	107.53	23.94	3.98
E	7.78	244.95	82.99	51.51	158.57	85.93	26.64	3.87
F	7.64	254.95	94.71	49.90	145.88	86.27	30.17	3.27
G	7.71	249.79	93.22	50.70	143.13	107.53	28.14	4.29
H	7.59	244.88	93.02	49.03	142.44	86.27	34.62	3.90
I	7.60	241.57	103.23	48.08	156.27	95.80	35.91	3.07
J	7.62	243.29	113.08	49.03	150.87	108.27	44.18	3.66

3.1. Diurnal Variation in Concentration of Iron at All Hotspot Locations on GVC

Difference in the concentration of iron between the samples from the upstream to the downstream end was observed in all samples collected from the GVC hotspots. The iron concentrations from these samples ranged from 1.29 ppm to 8.16 ppm. The maximum, minimum, standard deviation, variance and mean concentrations of iron across all the diurnal samples are shown in Table 4. All the measured values were above the approved limit for iron concentration [7], indicating the impact of pollution on the GVC at all time periods and across all hotspots.

Table 4. Statistics summary of iron concentration at each hotspot.

Station Code	Iron Concentration in ppm				Variance
	Max	Min	Mean	Standard Deviation	
A	2.29	1.49	1.88	0.31	0.10
B	2.76	1.69	2.02	0.35	0.12
C	2.63	1.36	1.80	0.40	0.16
D	2.09	1.63	1.90	0.18	0.03
E	2.23	1.83	2.08	0.14	0.02
F	2.36	1.29	1.81	0.36	0.13
G	8.17	2.29	3.77	1.89	3.59
H	3.56	2.03	2.37	0.53	0.29
I	3.56	2.23	2.77	0.46	0.21
J	4.50	2.96	3.78	0.55	0.30

Anthropogenic activities during the peak hours of the day are evident from the graphs shown in Figures 4 and 5. The diurnal variation from the forenoon sampling to the afternoon sampling marked the culmination of iron contamination from various agricultural, aquacultural and industrial sources [11]. Iron levels were found to be higher in the samples

taken in the afternoon compared to those taken earlier, as sunlight-driven chemical reactions in water help keep the iron redox cycle going by switching between ferric ion and ferrous ion forms [39]. The findings also highlight the impact of various anthropogenic sources on iron contamination at station 'G' during the diurnal times GT2 and GT4. The quick surge in iron concentration might be due to the extensive washing of vehicles, as vehicle washing activities and the body parts of vehicles, such as brakes, tyres, and outer body frames, yield iron [42]. The highest levels of iron contamination were observed at the downstream end of the GVC at all diurnal times. Station 'J' experienced variations in iron concentration from T1 to T6; these variations could be due to the culmination of all the upstream-side pollution along with the excess poultry, hatchery, agricultural, and aquacultural discharges entering as non-point sources of pollution into the GVC stream [4], as it is located at the tail-end portion of the canal. High dietary iron levels in aquaculture ponds and culture tanks can lead to direct excretion through feces, without absorption through the gut wall, or can be transferred to the fish gills and released into water as a pollutant [43]. The concentration of iron is comparatively low at T1 across all sampling stations; this could be due to the inactivity of anthropogenic sources during the early hours of the diurnal cycle, which could be an ideal time for municipalities and panchayats to draw water from the canals to prevent high iron levels in drinking water and reduce high water treatment and maintenance costs. Suceava city, situated between the selected monitoring points, showed significantly altered shapes and hourly positions of the diurnal cycles of the same parameter [44], highlighting the significant changes in the monitored water parameters. The variations in iron concentration at different times indicate the importance of diurnal variation over seasonal variation. Along with the iron concentration in the samples, other heavy metals like cadmium, copper, manganese and zinc were determined. The results showed that the majority of samples fall below the permissible range (no threat) of their standard concentrations and hence their effect on iron adsorption is omitted in this study.

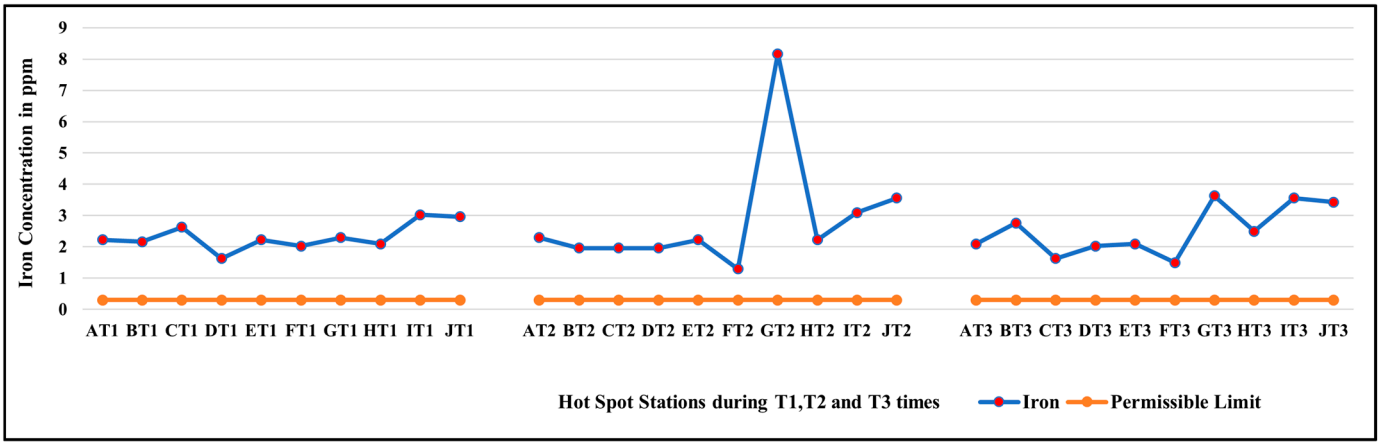


Figure 4. Diurnal variation of iron concentration in forenoon samples from all hotspots.

3.2. Comparative Iron Removal Efficiency: Static vs. Agitated Green Stem Biomass

Green stem biomass (GSB) of *T. cordifolia* represents the living part of the plant stem; the surface of the living plant stem binds the metal ions or absorbs them through its own metabolic process, which is crucial for the removal of pollutants [1]. This was tested in the laboratory under static and agitated conditions to understand the biosorption capabilities of the plant biomass. The standard iron sample interacted closely with the plant biomass during this process, as agitation helped mix them better and improved the results of iron detection in a turbulent flow-type condition. Toxic damage to plant biomass can occur due to increased metal concentration, but plants eventually undergo chemical damage control

as an immediate response [21], so the fittest plant can effectively remediate the toxicity impact. In the agitated biomass combinations, biosorption was dependent on contact time: the initial 25 min of iron detection showed a reduction in iron concentration, which might be due to the absorption of iron by the plant biomass; however, between 25 and 40 min, the green stem began releasing iron from its biomass, increasing the concentration of iron, as indicated in Figure 6. Metal ions in the solution increase the percentage of saturation, leading to a decrease in biosorption rate over time [25]. Subsequently, a reduction in iron concentration was observed from all three combinations of GSB after 40 min. A more stable removal efficiency was observed in GSB-2 compared to GSB-1. GSB-3 showed better removal efficiency than GSB-1 and GSB-2. This could be due to the higher availability of plant biomass in its composition. As the concentration of biomass increases, the number of possible binding regions also increases, increasing the percentage removal efficiency [20]. This suggests that the effectiveness of GSB in removing iron during agitation is dependent on the amount of biomass present in the sample. The overall iron removal efficiency of green stem biomass in standard iron is ranked as GSB-3 > GSB-2 > GSB-1 in agitation.

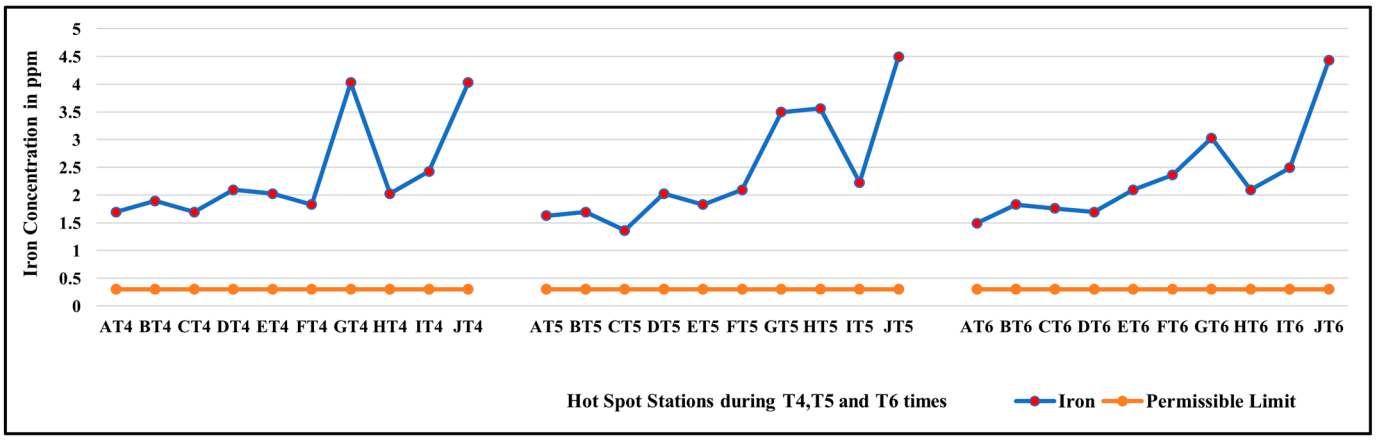
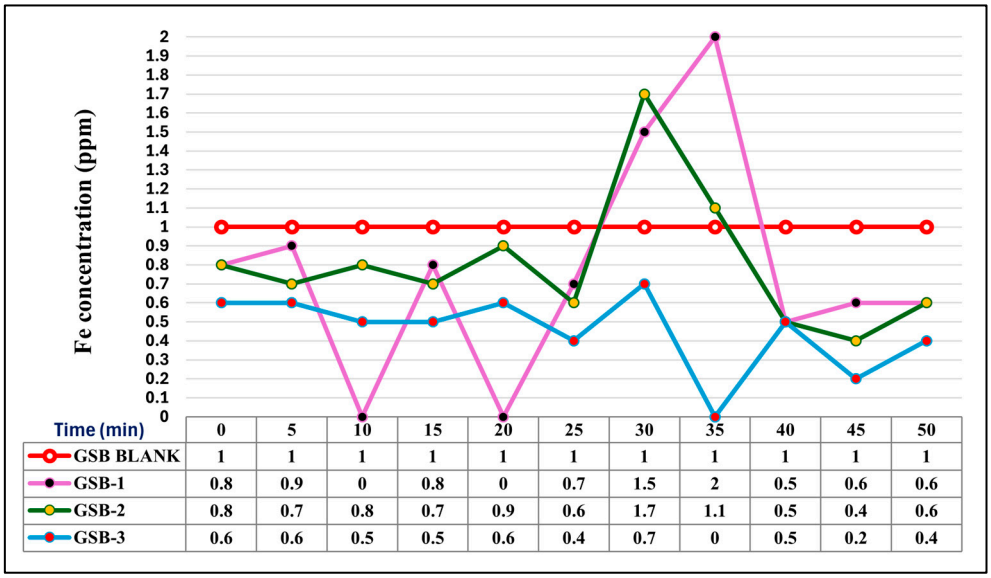


Figure 5. Diurnal variation of iron concentration in afternoon samples from all hotspots.

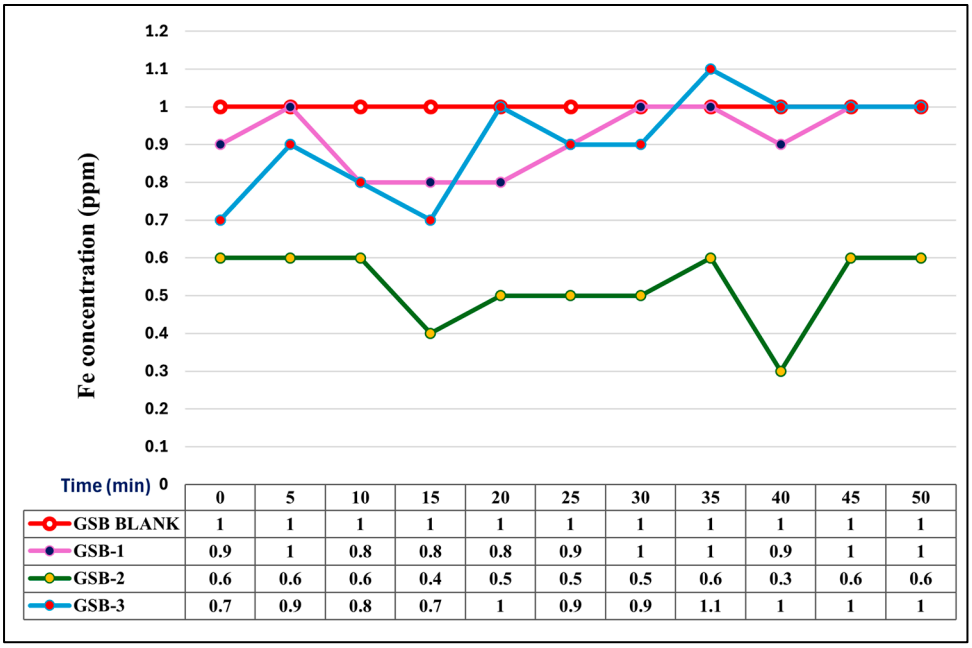
The interaction between the standard iron sample and the plant biomass in GSB without agitation (static) was slightly slower compared to agitated biomass, but the real characteristics of the plant biomass in this stable condition were seen. By following a certain incubation period, equilibrium is achieved, after which the biosorbent gets separated [25]. The quantity of GSB greatly influences the biosorption of iron by the plant biomass. GSB-2 showed greater biosorption capability (i.e., 50%) compared to GSB-1 and GSB-3, as shown in Figure 7. Studies showed that there could be an increase in biosorption before the system reaches its equilibrium condition [26]. Despite having a lower biomass weight in its composition than GSB-3, GSB-2 demonstrated greater biosorption capability. The overall iron removal efficiency of green stem biomass in standard iron is ranked as GSB-2 > GSB-1 > GSB-3 in static conditions.

Despite having variations in the biosorption capabilities in static and agitated biomass, *T. cordifolia* creepers could be grown on the flowing and stagnant water bodies, which could effectively remove iron contamination similar to floating treatment wetlands (FTWs) [19,24]. These plants offer potential natural and cost-effective solutions for traditional heavy metal treatment processes and can improve water quality.



Time (min)	0	5	10	15	20	25	30	35	40	45	50
GSB BLANK	1	1	1	1	1	1	1	1	1	1	1
GSB-1	0.8	0.9	0	0.8	0	0.7	1.5	2	0.5	0.6	0.6
GSB-2	0.8	0.7	0.8	0.7	0.9	0.6	1.7	1.1	0.5	0.4	0.6
GSB-3	0.6	0.6	0.5	0.5	0.6	0.4	0.7	0	0.5	0.2	0.4

Figure 6. Iron removal efficiency of *T. cordifolia* green stem biomass with agitation.

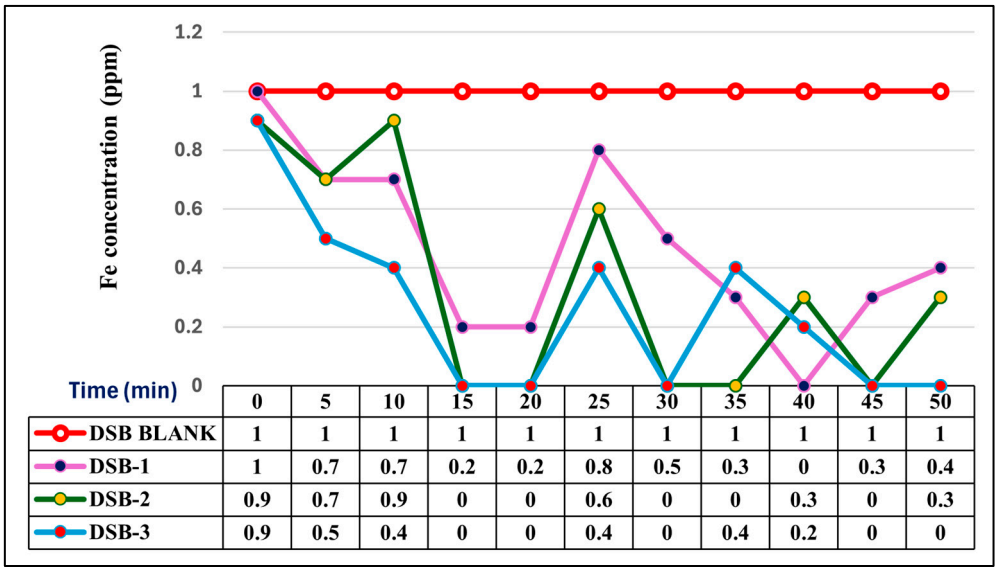


Time (min)	0	5	10	15	20	25	30	35	40	45	50
GSB BLANK	1	1	1	1	1	1	1	1	1	1	1
GSB-1	0.9	1	0.8	0.8	0.8	0.9	1	1	0.9	1	1
GSB-2	0.6	0.6	0.6	0.4	0.5	0.5	0.5	0.6	0.3	0.6	0.6
GSB-3	0.7	0.9	0.8	0.7	1	0.9	0.9	1.1	1	1	1

Figure 7. Iron removal efficiency of *T. cordifolia* green stem biomass without agitation.

3.3. Comparative Iron Removal Efficiency: Static vs. Agitated Dry Stem Biomass

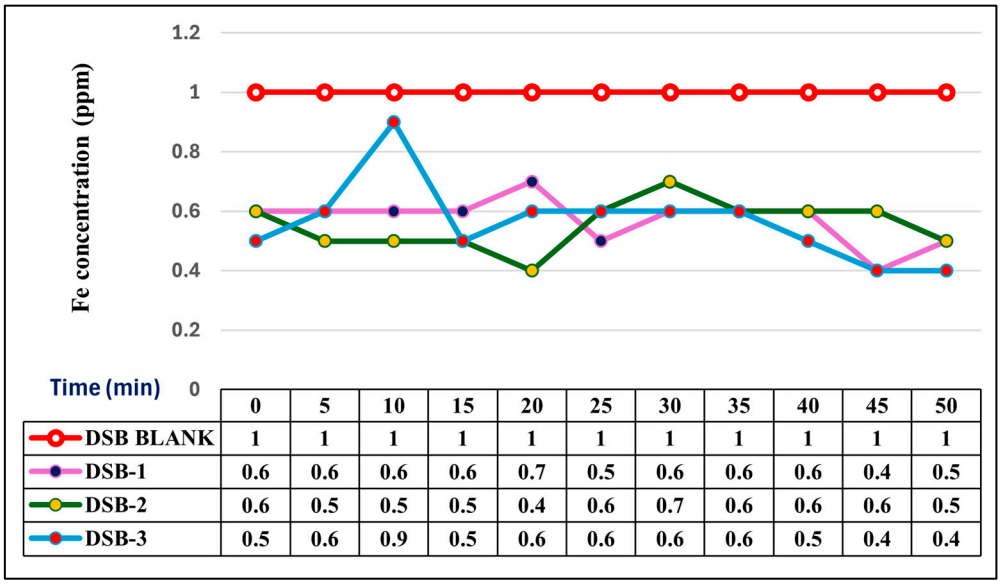
Dry stem biomass (DSB) of *T. cordifolia* represents the dead part of the plant stem. This biomass combination demonstrates the biosorption efficiency of the plant at the end of its life cycle. Dead plant material is widely believed to be a potential method for removing heavy metals from polluted water [1]. The results show that DSB with agitation had better iron biosorption capabilities than GSB in the standard iron samples with agitation, due to the availability of more pores in the dry plant biomass, as they take in more iron instead of letting it go into the sample. The fluctuations in the iron absorption capabilities were found to be below the permissible level of iron in drinking water in a few instances and below the sample blank during all 5 min intervals in all DSB combinations, as shown in Figure 8. The effectiveness of iron removal is ranked as DSB-3 > DSB-2 > DSB-1 under agitation.



Time (min)	0	5	10	15	20	25	30	35	40	45	50
DSB BLANK	1	1	1	1	1	1	1	1	1	1	1
DSB-1	1	0.7	0.7	0.2	0.2	0.8	0.5	0.3	0	0.3	0.4
DSB-2	0.9	0.7	0.9	0	0	0.6	0	0	0.3	0	0.3
DSB-3	0.9	0.5	0.4	0	0	0.4	0	0.4	0.2	0	0

Figure 8. Iron removal efficiency of *T. cordifolia* dry stem biomass with agitation.

DSB without agitation showed greater biosorption capabilities (i.e., >60%) in all its compositions. In comparison with DSB with agitation, DSB without agitation always showed consistent biosorption of iron. This could be due to the static nature of the plant biomass leading to fewer fluctuations in the absorption of iron, as shown in Figure 9. The major outcome of this biomass combination is that the plant creeper can be utilized in field applications, like pond cleanup or removal of heavy metals in stagnant and polluted water bodies [25,26]. The effectiveness of iron removal is ranked equal in all three static cases, DSB-1/2/3.



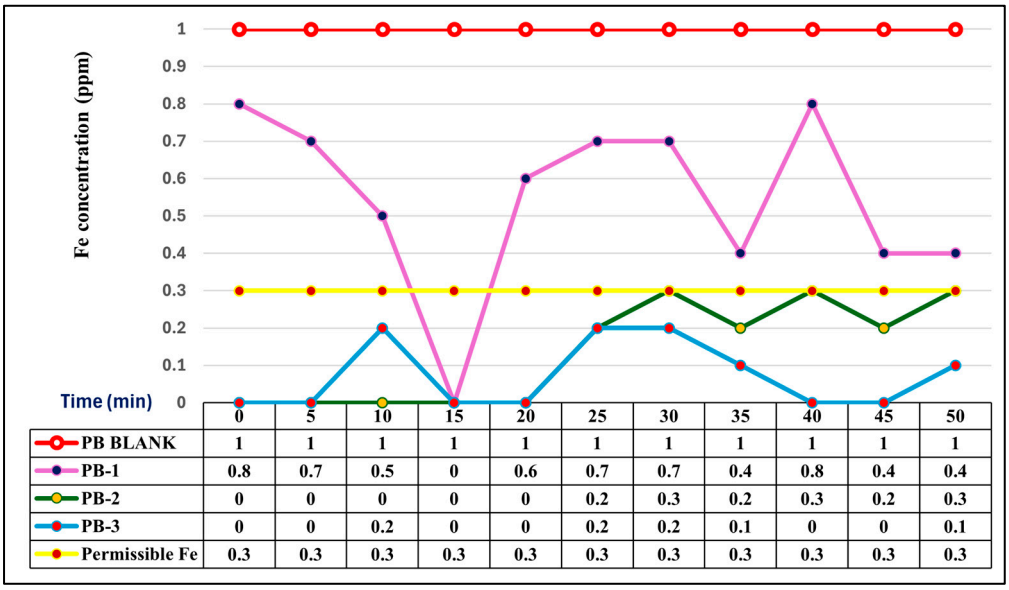
Time (min)	0	5	10	15	20	25	30	35	40	45	50
DSB BLANK	1	1	1	1	1	1	1	1	1	1	1
DSB-1	0.6	0.6	0.6	0.6	0.7	0.5	0.6	0.6	0.6	0.4	0.5
DSB-2	0.6	0.5	0.5	0.5	0.4	0.6	0.7	0.6	0.6	0.6	0.5
DSB-3	0.5	0.6	0.9	0.5	0.6	0.6	0.6	0.6	0.5	0.4	0.4

Figure 9. Iron removal efficiency of *T. cordifolia* dry stem biomass without agitation.

Studies suggest that aquatic plants like *Eichhornia crassipes* (*water hyacinth*), *Carex pseudo Cyperus*, *Water lettuce*, and *Duckweed* [19,23,24] show better hyperaccumulation of heavy metals in their early stage, but at the end of their life cycle, they tend to become dead waste or weeds, that pollute the medium in which they are grown. Water hyacinth has been listed among the world's worst aquatic weeds [45]. In comparison, *T. cordifolia* demonstrated greater absorption across all biomass combinations in DSB, indicating maximum potential in its completely dried form.

3.4. Comparative Iron Removal Efficiency: Static vs. Agitated Powder Biomass

Powder biomass (PB) of *T. cordifolia* is the extracted powder form of the green plant stem. It is made from the starch of *T. cordifolia* and is mainly called 'Guduchi satva' which is used in traditional medicine to treat various health issues [33,37]. PB with agitation offered the best removal efficiency of iron among all other *T. cordifolia* biomass combinations of GSB and DSB with agitation. Since the surface area of spread is more than the green and dry biomass, powder biomass exhibited the highest biosorption efficiency of iron [16]. PB-2 and PB-3 almost neutralized the standard iron sample (4ppm), and their values were far below the standard permissible levels of iron in drinking water, as shown in Figure 10. The initial removal efficiency using biomass powder was higher than the initial rate with green plant biomass, due to the external particle transfer and intraparticle diffusion [18]. In agitated conditions, the effectiveness of iron removal ranks as PB-3 > PB-2 > PB-1, indicating that the higher the biomass, the higher the biosorption [22]. The powdered biomass is useful for the treatment of wastewater and industrial effluents [16], and hence, it could be effective not only in removing iron, but also in reducing other major pollutants present in surface water bodies and wastewater treatment plants.



Time (min)	0	5	10	15	20	25	30	35	40	45	50
PB BLANK	1	1	1	1	1	1	1	1	1	1	1
PB-1	0.8	0.7	0.5	0	0.6	0.7	0.7	0.4	0.8	0.4	0.4
PB-2	0	0	0	0	0	0.2	0.3	0.2	0.3	0.2	0.3
PB-3	0	0	0.2	0	0	0.2	0.2	0.1	0	0	0.1
Permissible Fe	0.3	0.3	0.3	0.3	0.3	0.3	0.3	0.3	0.3	0.3	0.3

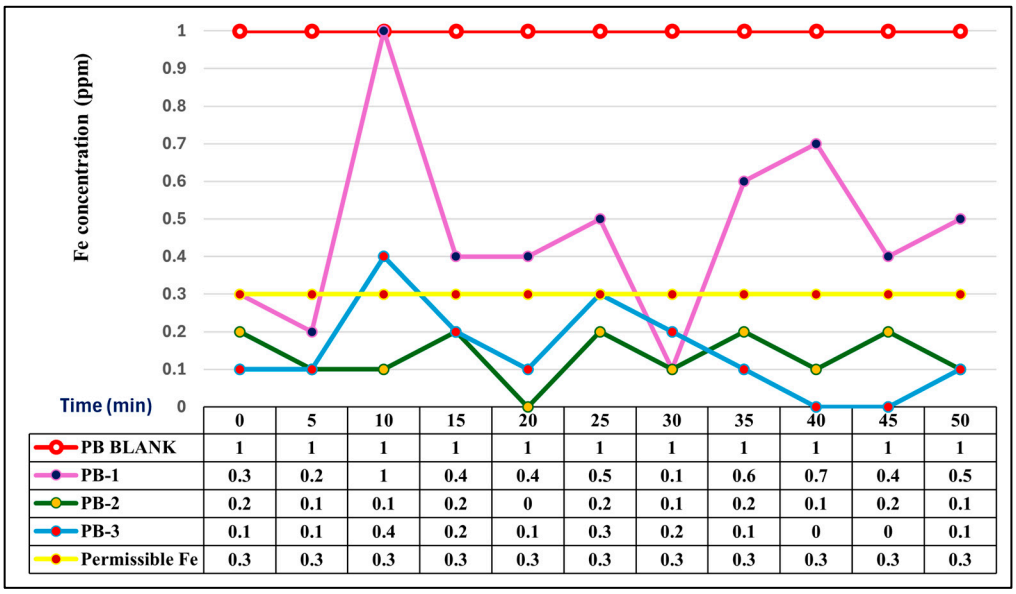
Figure 10. Iron removal efficiency of *T. cordifolia* powder biomass with agitation.

PB without agitation offered better removal efficiency of iron with respect to the contact time, as the powdered biomass was in the suspended state for most of the time. The fluctuations in the biosorption of iron in PB-1 might be due to the lower concentration of powdered biomass. PB-2 and PB-3 neutralized the standard iron sample below the standard permissible levels of iron, as shown in Figure 11. This strengthens the application of PB in stagnant and polluted water bodies. The biomass powder has proved to be effective in adsorbing heavy metals like lead (Pb) from various metal ions and anions, along with iron (358 mg g^{-1}) [16], which is very efficient and on par with other systems reported recently. The effectiveness of iron removal is ranked as PB-3 > PB-2 > PB-1, without agitation.

3.5. Equilibrium Times of T. cordifolia Biomass

The equilibrium times of the samples loaded with GSB, DSB, and PB for the removal of iron were obtained between 40 and 50 min. The plant biomass of *T. cordifolia*, which contains iron in its composition [46], adsorbed the iron present in the sample during the first 25 min but then released it back into the sample between 25 and 40 min. Thereafter, a stable sorption of iron occurred from 40 to 50 min [16], and the concentration of iron

remained stable thereafter. So, all the samples were tested for iron sorption for a period of 50 min, with a 5 min time interval. The iron sorption rate increased with the increase in the concentration of biomass, except for GSB without agitation; this could be due to the slower reaction of the green stem with the iron in samples.



Time (min)	0	5	10	15	20	25	30	35	40	45	50
PB BLANK	1	1	1	1	1	1	1	1	1	1	1
PB-1	0.3	0.2	1	0.4	0.4	0.5	0.1	0.6	0.7	0.4	0.5
PB-2	0.2	0.1	0.1	0.2	0	0.2	0.1	0.2	0.1	0.2	0.1
PB-3	0.1	0.1	0.4	0.2	0.1	0.3	0.2	0.1	0	0	0.1
Permissible Fe	0.3	0.3	0.3	0.3	0.3	0.3	0.3	0.3	0.3	0.3	0.3

Figure 11. Iron removal efficiency of *T. cordifolia* powder biomass without agitation.

3.6. Diurnal Variation in Iron Removal Efficiency of Optimized T. cordifolia Biomass Combinations for Sustainable Surface Water Treatment

The optimal biomass evaluation uses diurnal samples from GVC whose iron concentration is known. The diurnal samples are taken from a flowing canal, which is important for the evaluation process. A mix of ideal biomass types (GSB-3, DSB-3, and PB-3) in a turbulent flow (agitated condition) from Sections 3.2–3.4 are selected to see how effectively they can optimize the iron concentration in the diurnal samples. The removal efficiency of iron in each sample, starting from the upstream end of the GVC and working downstream, is checked. The mean removal efficiency is considered for evaluation of each sample at all diurnal times.

Compared to DSB-3 and GSB-3, the removal efficiency of iron in all the diurnal samples from the extracted powder biomass (PB-3) with agitation was observed to be very high across all the samples (Figures 12–17). This could be due to the quick biosorption capability of the powder biomass with the iron concentration present in the samples [20], A similar pattern of iron removal efficiency was observed at all diurnal times starting from T1 to T6 at all hotspot stations. DSB-3 and GSB-3 showed lesser iron removal efficiencies when compared to PB-3. A mean iron removal efficiency of 51.97% was observed across all the hotspot sample stations, irrespective of the biomass combinations. PB-3 with agitation showed better iron removal efficiency compared to GSB-3 and DSB-3 in all hotspot samples, achieving the highest removal rate of 100% and a mean of 72.43% (±15.84 SD). DSB-3 showed a maximum efficiency of 72.45% and a mean of 41.77% (±13.59 SD). In comparison, GSB-3 demonstrated a maximum efficiency of 67.56% and an average of 35.32% (±12.9 SD), as illustrated in Table 5. The powdered biomass of *T. cordifolia* (PB-3) achieved an iron removal efficiency double that of green stem and dry stem biomass. The variability (SD of 15.84) of PB-3 indicated its sensitivity to operational conditions. PB-3 exhibited superior iron removal capabilities even under suboptimal conditions, with a minimum efficiency value of 26.87%, when compared with DSB-3 (18.26%) and GSB-3 (12.88%). The effective removal efficiency follows the order of PB-3 > DSB-3 > GSB-3. With the simultaneous

increase in the concentration of iron and TDS (total dissolved solids), the biosorption capability of *T. cordifolia* decreased. This phenomenon was observed at stations GT2, GT3, GT4, GT5, GT6, JT4, JT5, JT6, HT5, and ET3. On the other hand, the decrease in TDS concentration improved the biosorption capability of *T. cordifolia* in removing iron. This was observed at the upstream hotspot stations A and B, which indicates that the removal efficiency of *T. cordifolia* was dependent on the concentration of iron and TDS present in the sample. These results on the entire stretch of GVC demonstrate a simple, sustainable and optimized solution for the removal of heavy metal iron using an eco-friendly *T. cordifolia* biomass at all diurnal times.

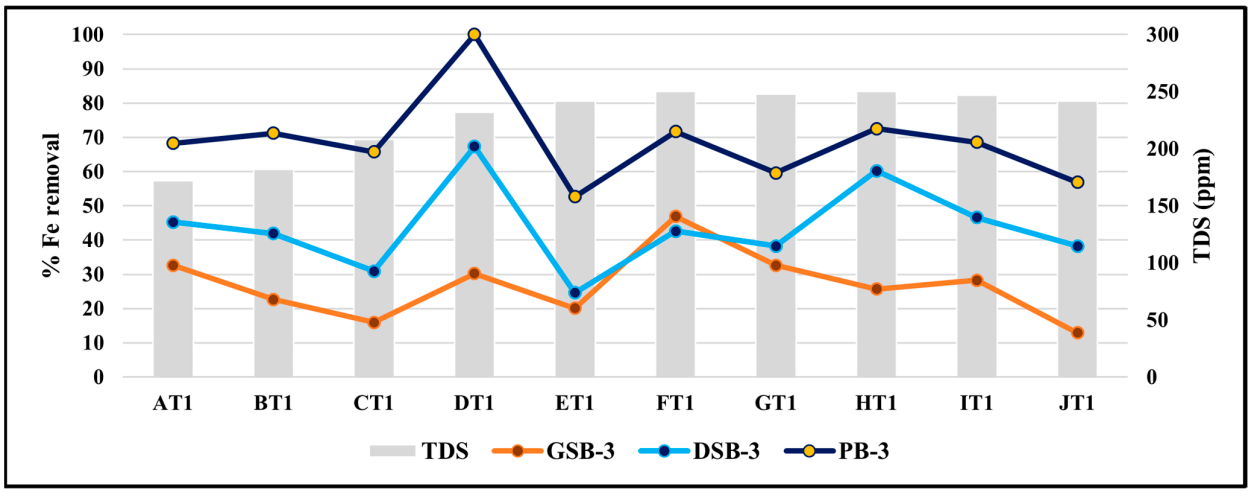


Figure 12. Percentage iron removal by *T. cordifolia* plant biomass from GVC samples at diurnal time T1.

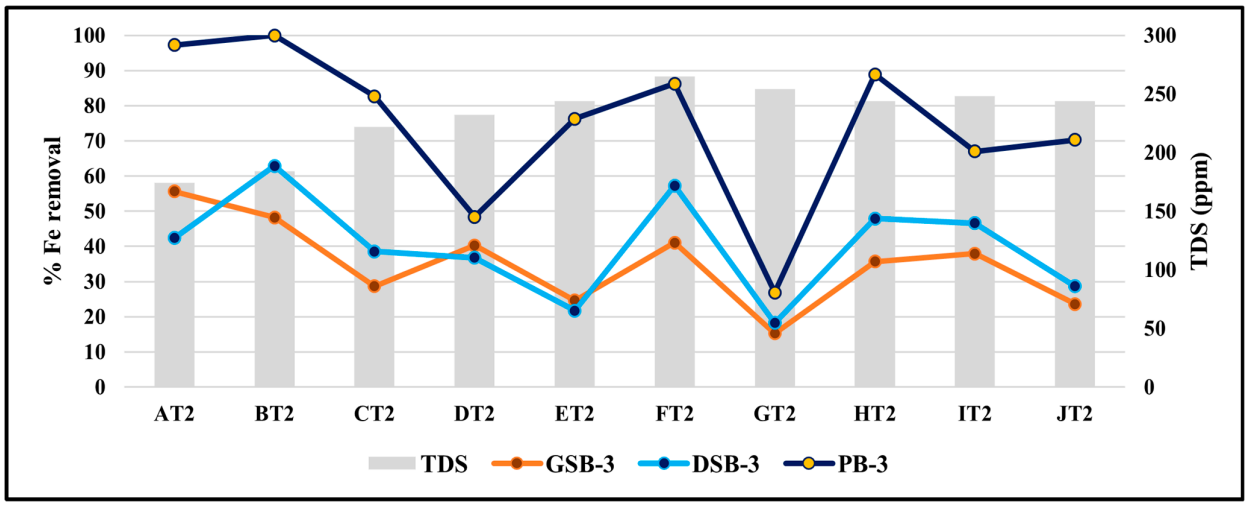


Figure 13. Percentage iron removal by *T. cordifolia* plant biomass from GVC samples at diurnal time T2.

Table 5. Descriptive statistics of diurnal GVC samples by *T. cordifolia* biomass.

TC Biomass (with Agitation)	(%) Iron Removal Efficiency (R_e) in Diurnal GVC Samples			
	Max	Min	Mean	Standard Deviation
GSB-3	67.56	12.88	35.32	12.9
DSB-3	72.45	18.26	41.77	13.59
PB-3	100	26.87	72.43	15.84

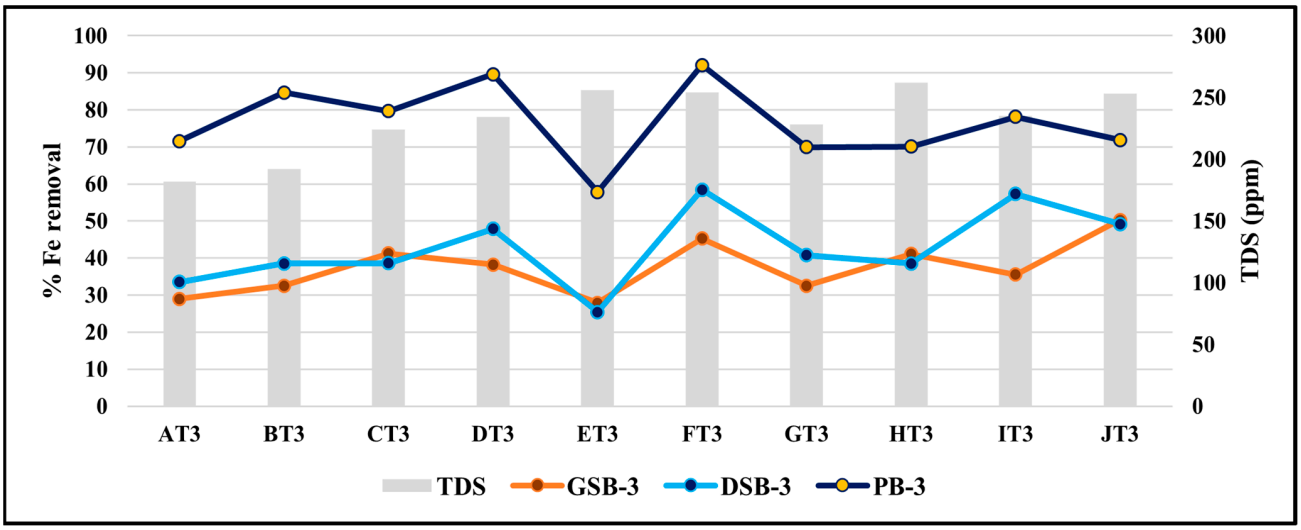


Figure 14. Percentage iron removal by *T. cordifolia* plant biomass from GVC samples at diurnal time T3.

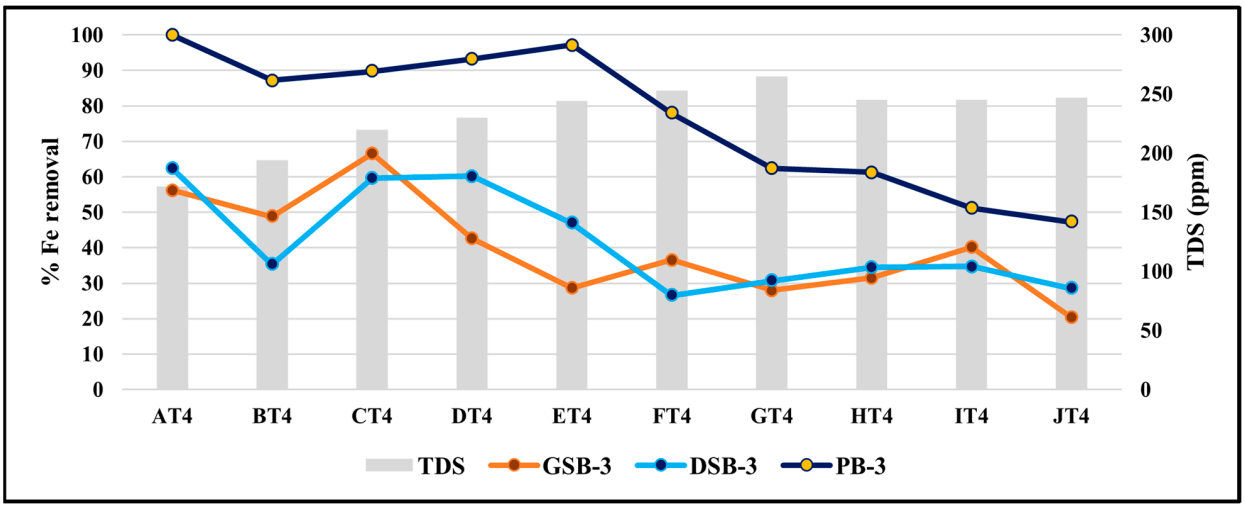


Figure 15. Percentage iron removal by *T. cordifolia* plant biomass from GVC samples at diurnal time T4.

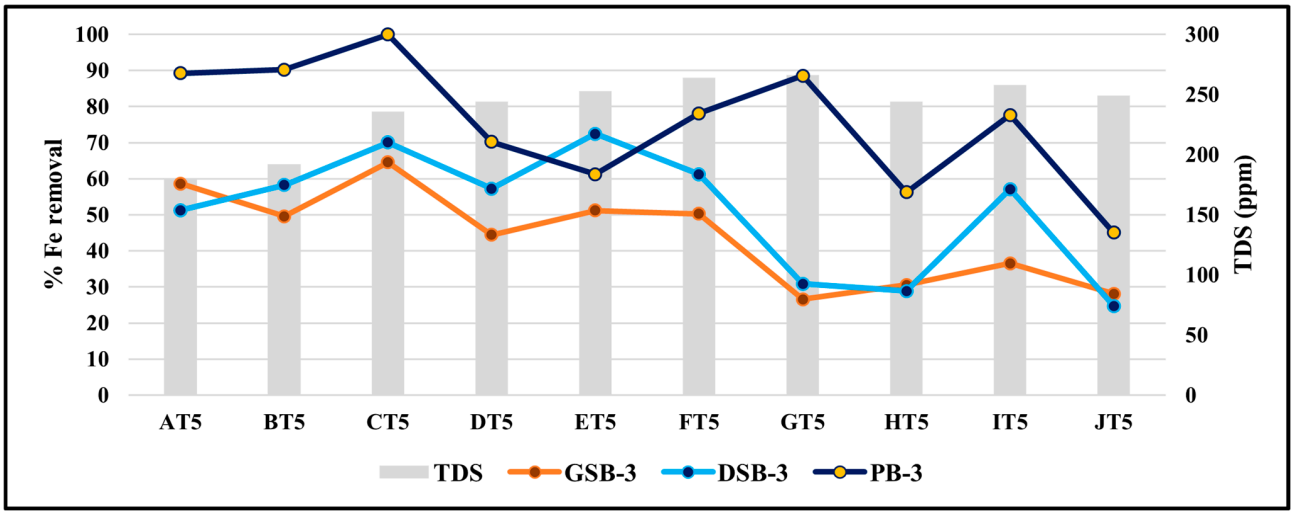


Figure 16. Percentage iron removal by *T. cordifolia* plant biomass from GVC samples at diurnal time T5.

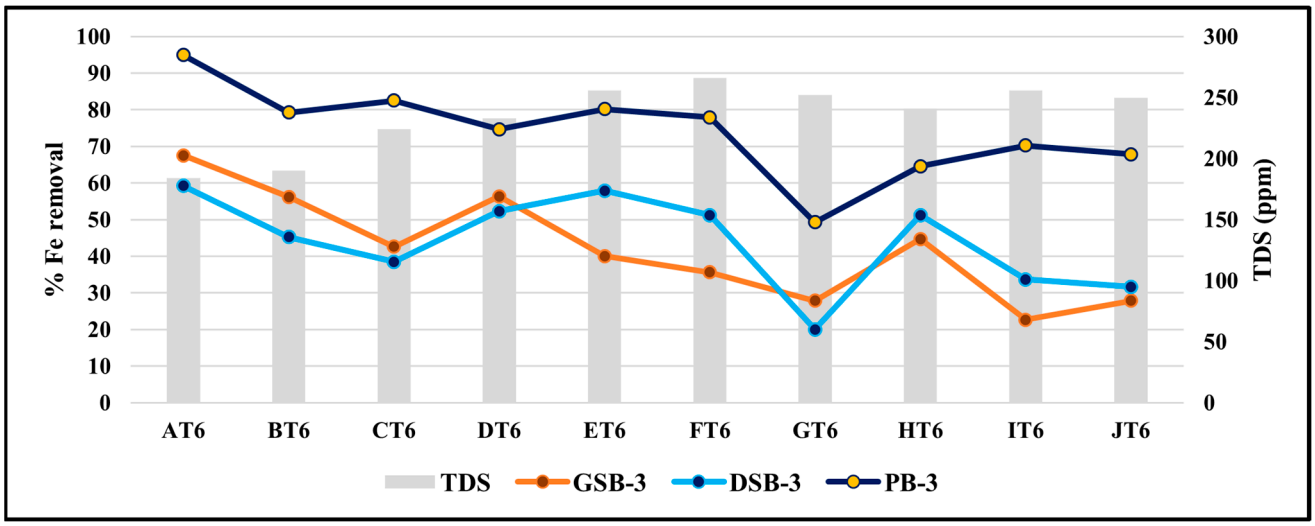


Figure 17. Percentage iron removal by *T. cordifolia* plant biomass from GVC samples at diurnal time T6.

3.7. Cumulative Removal Efficiency of Iron by T. cordifolia Biomass at Upstream, Midstream and Downstream Diurnal Samples on GVC

The development of sustainable management strategies requires the identification and quantification of pollution sources [4]. The culmination of pollution from the upstream of the canal and unprecedented non-point sources of pollution impacted the removal efficiency of iron by *T. cordifolia* biomass combinations, as shown in Figure 18. The cumulative iron removal efficiency of all the upstream samples is significantly higher than that of the midstream and downstream samples. This surge could be due to the culmination of anthropogenic pollution starting at hotspot station 'B'. At this point, the pollution sources are an amalgamation of domestic sewage, poultry, industrial, and agricultural discharges coming from Velivennu town, increasing the midstream and downstream pollution load. At station 'G', because of the increased anthropogenic activity during the day, there was a higher level of TDS, which affected the removal efficiency of iron.

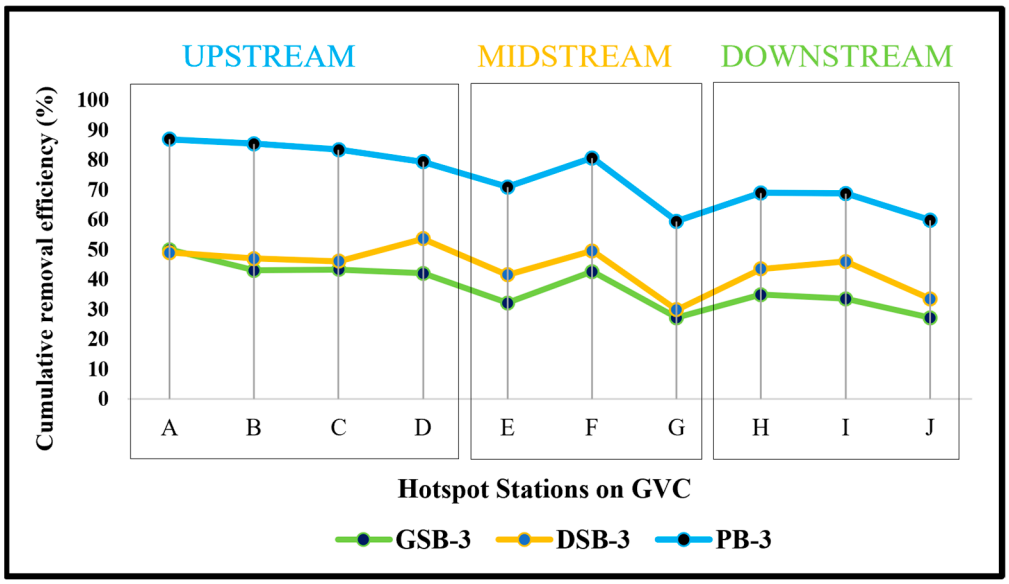


Figure 18. Cumulative iron removal efficiency of *T. cordifolia* biomass combinations.

3.8. Effect of TDS on the Removal Efficiency of Iron

In all the samples from upstream to downstream GVC, a variation in TDS was observed. A maximum TDS of 266 ppm was observed at GT5, and a minimum TDS of 172 ppm was observed at AT1 and AT4. The removal efficiency of TC biomass decreased with an increase in TDS and iron concentration in GVC water samples. This effect was observed in the diurnal samples at the downstream end; at hotspot GT2, the TDS concentration was 254 ppm and the iron concentration was 8.17 ppm (highest among all the diurnal samples); the biomass of GSB-3, DSB-3 and PB-3 with agitation only managed to absorb 15.28%, 18.26% and 26.87% of iron, respectively, indicating the effect of TDS and iron concentration on removal efficiency. Similar variations were observed at stations I and J. Similarly, with the decrease in TDS levels, the rate of iron absorption from TC biomass increased in the samples on the upstream side of GVC at stations A and B.

3.9. Effect of T. cordifolia Creepers Grown on GVC

Visual observations revealed that few hotspot locations had a larger spread of *T. cordifolia* creepers, extending from the banks and spreading across the canal. At station 'C', despite having multiple pollution sources, diurnal samples showed lower levels of iron concentration. This phenomenon was observed between stations B and D during the time periods T3, T4, and T5 as shown in Figure 19. The canal path at station C was covered by *T. cordifolia* creepers, which could be a potential cause for the decrease in iron concentration located between stations B and D. The results from the TC biomass combinations (DSB-3 and GSB-3) can be attributed to these reduced iron concentrations. The decrease in iron concentration that occurred during the forenoon session of diurnal sampling might indicate a correlation between temperature and iron absorption by *T. cordifolia* plants.

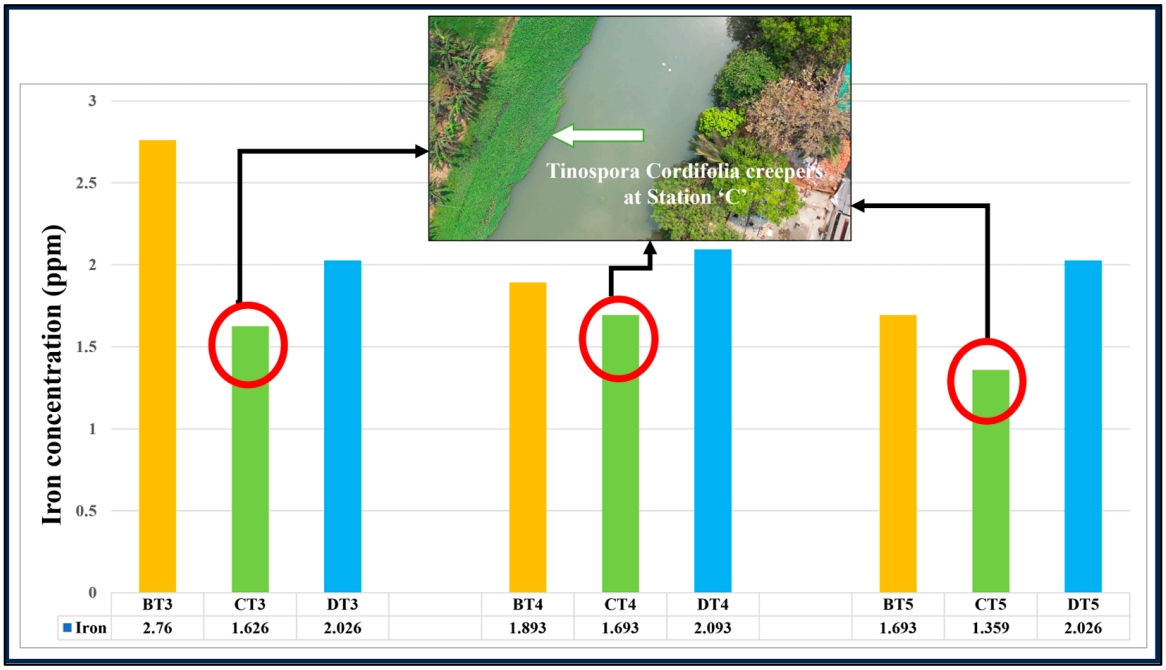


Figure 19. Reduction in iron concentration at hotspot 'C' on GVC.

As *T. cordifolia* is a creeper with fast growth, it can be effectively used across the stretch of the GVC to reduce the heavy metal loads in the canal. As demonstrated in Sections 3.2 and 3.3, the plant can also be used in live and dead forms for the biosorption of heavy metal iron.

3.10. Fate and Disposal of Iron-Loaded T. cordifolia Biomass

The iron-loaded biomass obtained from the biosorption process is dried under a shade at an ambient temperature of 25–30 °C for a span of 1–2 weeks to remove the moisture content. The biomass is then oven-dried at a temperature of 60 °C for a duration of 24 h to remove the remaining moisture content. The dried biomass is then moved to a muffle furnace, where the biomass is heated to a temperature ranging between 500 and 600 °C in the absence of oxygen and converted into biochar. The obtained biochar is rich in iron content, which is a very essential element for class F fly ash used in concrete. This biochar can be used as a partial replacement for cement in concrete production [47].

4. Conclusions

In this study, the biosorption of iron from a surface water canal is achieved naturally using *T. cordifolia* biomass through its life cycle in green stem, dry stem, and powder forms. All three optimized biomass combinations showed the best removal of iron, in the order of PB-3 > DSB-3 > GSB-3. The removal efficiency increased with the increase in the biomass concentration. The biosorption ability of powder biomass is greater than that of green and dried stem biomass, indicating its applicability in water bodies, water treatment plants, and sensitive zones with high levels of iron contamination. The biosorption of iron by green and dry stem biomass is comparatively less effective than that of powdered biomass; however, it can be used as a natural biosorbent in flowing and stagnant water bodies where human intervention or accessibility is challenging. The plant's availability, applicability, and quick growth in an aqueous medium make it a desirable and cost-effective alternative for biosorption of iron. Although this study evaluated the iron biosorption of iron by T. cordifolia biomass (life cycle), the method can be applied to validate the biosorption of other heavy metals like Hg, Cd, Mn, Cu and Pb in water bodies.

Supplementary Materials: The following supporting information can be downloaded at: https://www.mdpi.com/article/10.3390/w17203020/s1; Table S1. Descriptive statistics of all the stations.

Author Contributions: Conceptualization, P.R.; methodology, P.R.; validation, P.R., F.E.E. and P.R.R.; formal analysis, P.R.; investigation, P.R. and T.B.S.; resources, P.R.R.; data curation, T.B.S.; writing—original draft preparation, P.R.; writing—review and editing, P.R., F.E.E., R.K.C. and P.R.R.; visualization, P.R.; supervision, F.E.E.; funding acquisition, R.K.C. All authors have read and agreed to the published version of the manuscript.

Funding: This work was supported by the BRIDGE Project (funded by RCN, Norway; Project No. 322325) at UiT The Arctic University of Norway. Publication charges for this article were covered by a grant from the publication fund of UiT The Arctic University of Norway.

Data Availability Statement: The original contributions presented in this study are included in the article/Supplementary Material. Further inquiries can be directed to the corresponding author.

Acknowledgments: Authors acknowledge the support from BRIDGE Project at UiT. The laboratory facilities for conducting experimental work were provided by WET research centre and Department of Civil Engineering of SRKR Engineering college.

Conflicts of Interest: The authors declare no conflicts of interest.

References

1. Singh, V.; Ahmed, G.; Vedika, S.; Kumar, P.; Chaturvedi, S.K.; Rai, S.N.; Vamanu, E.; Kumar, A. Toxic heavy metal ions contamination in water and their sustainable reduction by eco-friendly methods: Isotherms, thermodynamics and kinetics study. *Sci. Rep.* **2024**, *14*, 7595. [CrossRef]
2. Hussain, J.; Husain, I.; Arif, M.; Gupta, N. Studies on heavy metal contamination in Godavari river basin. *Appl. Water Sci.* **2017**, *7*, 4539–4548. [CrossRef]

3. Aftab, A.; Aziz, R.; Ghaffar, A.; Rafiq, M.T.; Feng, Y.; Saqib, Z.; Rafiq, M.K.; Awan, M.A. Occurrence, source identification and ecological risk assessment of heavy metals in water and sediments of Uchalli lake—Ramsar site, Pakistan. *Environ. Pollut.* **2023**, *334*, 122117. [CrossRef] [PubMed]
4. Le, T.V.; Nguyen, B.T. Heavy metal pollution in surface water bodies in provincial Khanh Hoa, Vietnam: Pollution and human health risk assessment, source quantification, and implications for sustainable management and development. *Environ. Pollut.* **2024**, *343*, 123216. [CrossRef]
5. Zhang, X.Y.; Lin, F.F.; Wong, M.T.F.; Feng, X.L.; Wang, K. Identification of soil heavy metal sources from anthropogenic activities and pollution assessment of Fuyang County, China. *Environ. Monit. Assess.* **2009**, *154*, 439–449. [CrossRef]
6. Sharma, S.; Sharma, P.K. *Status of Trace and Toxic Metals in Indian Rivers*; River Data Directorate, Planning and Development Organisation, Central Water Commission: New Delhi, India, 2014.
7. *IS: 10500-2012*; Indian Standard-Drinking Water Specification (Second Revision). Bureau of Indian Standards: New Delhi, India, 2012.
8. WHO. *Iron in Drinking-Water*; WHO: Geneva, Switzerland, 2003.
9. WHO. *Guidelines for Drinking-Water Quality Third Edition Incorporating the First and Second Addenda, World Health Organization*; WHO Press: Geneva, Switzerland, 2008.
10. Baby, J.; Raj, J.S.; Biby, E.T.; Sankarganesh, P.; Jeevitha, M.; Ajisha, S.; Rajan, S.S. Toxic effect of heavy metals on aquatic environment. *Int. J. Biol. Chem. Sci.* **2010**, *4*, 939–952. [CrossRef]
11. Sarkar, A.; Shekhar, S. Iron contamination in the waters of Upper Yamuna basin. *Groundw. Sustain. Dev.* **2018**, *7*, 421–429. [CrossRef]
12. Jagapathi, R.M.; Penmetsa, R.R.; Muppidi, S.R.; Golla, S.B.; Kondepudi, N. Micro-Biological Contamination of Drinking Water in Western Delta of West Godavari District, Andhra Pradesh, India. *Int. Res. J. Environ. Sci.* **2016**, *5*, 1–5.
13. Abd Elnabi, M.K.; Elkaliny, N.E.; Elyazied, M.M.; Azab, S.H.; Elkhalifa, S.A.; Elmasry, S.; Mouhamed, M.S.; Shalamesh, E.M.; Alhorieny, N.A.; Abd Elaty, A.E.; et al. Toxicity of Heavy Metals and Recent Advances in Their Removal: A Review. *Toxics* **2023**, *11*, 580. [CrossRef]
14. Central Pollution Control Board. The Environment (Protection) Rules. In *General Standards for Discharge of Environmental Pollutants PART-A: Effluents*; Central Pollution Control Board: New Delhi, India, 1986.
15. Babu, K.; Nirmala, P.V. Heavy Metal Analysis in Agricultural Soils in Godavari River Basin of Rajahmundry Region, East Godavari District, Andhra Pradesh, India. *Curr. Agric. Res. J.* **2023**, *11*, 587–602. [CrossRef]
16. Vyas, G.; Bhatt, S.; Paul, P. Tinospora cordifolia derived biomass functionalized ZnO particles for effective removal of lead(ii), iron(iii), phosphate and arsenic(iii) from water. *RSC Adv.* **2019**, *9*, 34102–34113. [CrossRef]
17. Kandel, D.R.; Poudel, M.B.; Radoor, S.; Chang, S.; Lee, J. Decoration of dandelion-like manganese-doped iron oxide microflowers on plasma-treated biochar for alleviation of heavy metal pollution in water. *Chemosphere* **2024**, *357*, 141757. [CrossRef]
18. Halaimi, F.Z.; Kellali, Y.; Couderchet, M.; Semsari, S. Comparison of biosorption and phytoremediation of cadmium and methyl parathion, a case-study with live *Lemna gibba* and *Lemna gibba* powder. *Ecotoxicol. Environ. Saf.* **2014**, *105*, 112–120. [CrossRef]
19. Schück, M.; Greger, M. Plant traits related to the heavy metal removal capacities of wetland plants. *Int. J. Phytoremediation* **2020**, *22*, 427–435. [CrossRef]
20. Chandra Sekhar, K.; Kamala, C.T.; Chary, N.S.; Anjaneyulu, Y. Removal of heavy metals using a plant biomass with reference to environmental control. *Int. J. Miner. Process.* **2003**, *68*, 37–45. [CrossRef]
21. Sao, K.; Pandey, M.; Pandey, P.K.; Khan, F. Highly efficient biosorptive removal of lead from industrial effluent. *Environ. Sci. Pollut. Res. Int.* **2017**, *24*, 18410–18420. [CrossRef]
22. Abd-Elaal, A.-E.M.; Aboelkassem, A.; Gad, A.A.M.; Ahmed, S.A.S. Removal of heavy metals from wastewater by natural growing plants on River Nile banks in Egypt. *Water Pract. Technol.* **2020**, *15*, 947–959. [CrossRef]
23. Eid, E.M.; Shaltout, K.H.; Almuqrin, A.H.; Aloraini, D.A.; Khedher, K.M.; Taher, M.A.; Alfarhan, A.H.; Picó, Y.; Barcelo, D. Uptake prediction of nine heavy metals by *Eichhornia crassipes* grown in irrigation canals: A biomonitoring approach. *Sci. Total Environ.* **2021**, *782*, 146887. [CrossRef]
24. Arivukkarasu, D.; Sathyanathan, R. Floating wetland treatment an ecological approach for the treatment of water and wastewater—A review. *Mater. Today Proc.* **2023**, *77*, 176–181. [CrossRef]
25. Muddada, S.; Kanamarlapudi, S.L.R.; Chintalpudi, V.K. Application of Biosorption for Removal of Heavy Metals from Wastewater. In *Biosorption*; Derco, J., Vrana, B., Eds.; IntechOpen: Rijeka, Croatia, 2018.
26. Beni, A.A.; Esmaeili, A. Biosorption, an efficient method for removing heavy metals from industrial effluents: A Review. *Environ. Technol. Innov.* **2020**, *17*, 100503. [CrossRef]
27. Sharma, P.; Dwivedee, B.P.; Bisht, D.; Dash, A.K.; Kumar, D. The chemical constituents and diverse pharmacological importance of *Tinospora cordifolia*. *Heliyon* **2019**, *5*, e02437. [CrossRef]
28. Sharma, A.; Gupta, A.; Singh, S.; Batra, A. *Tinospora cordifolia* (*Willd.*) Hook. F. Thomson-A Plant Immense economic potential. *J. Chem. Pharm. Res.* **2010**, *2*, 327–333.

29. Subramanian, M.J.C.G.; Chattopadhyay, S. Antioxidant properties of a *Tinospora cordifolia* polysaccharide against iron-mediated lipid damage and γ-ray induced protein damage. *Redox Rep.* **2002**, *7*, 137–143. [CrossRef]
30. Upadhyay, A.K.; Kumar, K.; Kumar, A.; Mishra, H.S. *Tinospora cordifolia* (*Willd.*) Hook. f. and Thoms. (Guduchi) - validation of the Ayurvedic pharmacology through experimental and clinical studies. *Int. J. Ayurveda Res.* **2010**, *1*, 112–121. [CrossRef]
31. Choudhry, N.; Siddiqui, M.B.; Khatoon, S. Pharmacognostic evaluation of *Tinospora cordifolia* (*Willd.*) Miers and identification of biomarkers. *Indian J. Tradit. Knowl.* **2014**, *13*, 543–550.
32. Kumar, N.; Khatoon, S. Pharmacognostic Analysis of *Tinospora cordifolia* (*Thunb.*) Miers Respect Dioecy. *Single-Cell Biology.* **2019**, *7*, 1–10. [CrossRef]
33. Anu, C.; Rina, D.; Kiran, M.; Dinesh Kumar, M. Indian herb *Tinospora cordifolia* and *Tinospora* species: Phytochemical and therapeutic application. *Heliyon* **2024**, *10*, e31229. [CrossRef] [PubMed]
34. Singh, S.S.; Pandey, S.C.; Srivastava, S.; Gupta, V.S.; Patro, B.; Ghosh, A.C. Chemistry and medicinal properties of *Tinospora cordifolia* (*Guduchi*). *Indian J. Pharmacol.* **2003**, *35*, 83–91.
35. Pandey, P.; Pandey, M.; Sharma, R. Defluoridation of Water by a Biomass: *Tinospora cordifolia*. *J. Environ. Prot.* **2012**, *03*, 610–616. [CrossRef]
36. Rice, E.W.; Baird, R.B.; Eaton, A.D.; Clesceri, L.S. *Standard Methods for the Examination of Water and Wastewater*; American Public Health Association, American Water Works, Water Environment Federation: Washington, DC, USA, 2012.
37. Sharma, R.; Harisha, C.; Ruknuddin, G.; Prajapati, P. Quantitative estimation of Satva extracted from different stem sizes of *Guduchi* (*Tinospora cordifolia* (*Willd.*) Miers). *J. Pharm. Sci. Innov.* **2012**, *1*, 38–40.
38. Thakur, N.; Thakur, N. Removal of organic dyes and free radical assay by encapsulating polyvinylpyrrolidone and *Tinospora cordifolia* in dual (Co–Cu) doped TiO_2 nanoparticles. *Environ. Pollut.* **2023**, *335*, 122229. [CrossRef] [PubMed]
39. Rana, M.S.; Prajapati, S.K. Resolving the dilemma of iron bioavailability to microalgae for commercial sustenance. *Algal Res.* **2021**, *59*, 102458. [CrossRef]
40. Tamura, H.; Goto, K.; Yotsuyanagi, T.; Nagayama, M. Spectrophotometric determination of iron(II) with 1,10-phenanthroline in the presence of large amounts of iron(III). *Talanta* **1974**, *21*, 314–318. [CrossRef]
41. Singh, S. Spectroscopic determination of iron by 1,10-phenanthroline method. *Talanta* **2020**, *21*, 314–318.
42. Rai, R.; Sharma, S.; Gurung, D.B.; Sitaula, B.K. Heavy metal contamination in sediments from vehicle washing: A case study of Olarong Chhu Stream and Paa Chhu River, Bhutan. *Int. J. Environ. Stud.* **2019**, *76*, 66–83. [CrossRef]
43. Kasozi, N.; Tandlich, R.; Fick, M.; Kaiser, H.; Wilhelmi, B. Iron supplementation and management in aquaponic systems: A review. *Aquac. Rep.* **2019**, *15*, 100221. [CrossRef]
44. Briciu, A.-E.; Graur, A.; Oprea, D.I.; Filote, C. A Methodology for the Fast Comparison of Streamwater Diurnal Cycles at Two Monitoring Points. *Water* **2019**, *11*, 2524. [CrossRef]
45. Datta, A.; Maharaj, S.; Prabhu, G.N.; Bhowmik, D.; Marino, A.; Akbari, V.; Rupavatharam, S.; Sujeetha, J.A.R.P.; Anantrao, G.G.; Poduvattil, V.K.; et al. Monitoring the Spread of Water Hyacinth (*Pontederia crassipes*): Challenges and Future Developments. *Front. Ecol. Evol.* **2021**, *9*, 631338. [CrossRef]
46. Mahima; Rahal, A.; Prakash, A.; Verma, A.K.; Kumar, V.; Roy, D. Proximate and elemental analyses of *Tinospora cordifolia* stem. *Pak. J. Biol. Sci.* **2014**, *17*, 744–747. [CrossRef] [PubMed]
47. Aman, A.M.N.; Selvarajoo, A.; Lau, T.L.; Chen, W.-H. Biochar as Cement Replacement to Enhance Concrete Composite Properties: A Review. *Energies* **2022**, *15*, 7662. [CrossRef]

Disclaimer/Publisher's Note: The statements, opinions and data contained in all publications are solely those of the individual author(s) and contributor(s) and not of MDPI and/or the editor(s). MDPI and/or the editor(s) disclaim responsibility for any injury to people or property resulting from any ideas, methods, instructions or products referred to in the content.